



NRL/MR/6750--16-9682

On the Significance of a Carbon-Rich Background in Plasma-Based Graphene Oxide Reduction

M. BARAKET

National Research Council Postdoctoral Research Associate

Charged Particle Physics Branch

Plasma Physics Division

D.R. BORIS

Charged Particle Physics Branch

Plasma Physics Division

Z. WEI

P.E. SHEEHAN

Surface Chemistry Branch

Chemistry Division

S.G. WALTON

Charged Particle Physics Branch

Plasma Physics Division

June 2, 2016

REPORT DOCUMENTATION PAGE				Form Approved OMB No. 0704-0188	
Public reporting burden for this collection of information is estimated to average 1 hour per response, including the time for reviewing instructions, searching existing data sources, gathering and maintaining the data needed, and completing and reviewing this collection of information. Send comments regarding this burden estimate or any other aspect of this collection of information, including suggestions for reducing this burden to Department of Defense, Washington Headquarters Services, Directorate for Information Operations and Reports (0704-0188), 1215 Jefferson Davis Highway, Suite 1204, Arlington, VA 22202-4302. Respondents should be aware that notwithstanding any other provision of law, no person shall be subject to any penalty for failing to comply with a collection of information if it does not display a currently valid OMB control number. PLEASE DO NOT RETURN YOUR FORM TO THE ABOVE ADDRESS.					
1. REPORT DATE (DD-MM-YYYY) 02-06-2016		2. REPORT TYPE Memorandum Report		3. DATES COVERED (From - To)	
4. TITLE AND SUBTITLE On the Significance of a Carbon-Rich Background in Plasma-Based Graphene Oxide Reduction				5a. CONTRACT NUMBER	
				5b. GRANT NUMBER	
				5c. PROGRAM ELEMENT NUMBER	
6. AUTHOR(S) M. Baraket, ¹ D.R. Boris, Z. Wei, P.E. Sheehan, and S.G. Walton				5d. PROJECT NUMBER 67-4891-D6	
				5e. TASK NUMBER	
				5f. WORK UNIT NUMBER	
7. PERFORMING ORGANIZATION NAME(S) AND ADDRESS(ES) Naval Research Laboratory 4555 Overlook Avenue, SW Washington, DC 20375-5320				8. PERFORMING ORGANIZATION REPORT NUMBER NRL/MR/6750--16-9682	
9. SPONSORING / MONITORING AGENCY NAME(S) AND ADDRESS(ES) Office of Naval Research One Liberty Center 875 North Randolph Street, Suite 1425 Arlington, VA 22203-1995				10. SPONSOR / MONITOR'S ACRONYM(S) ONR	
				11. SPONSOR / MONITOR'S REPORT NUMBER(S)	
12. DISTRIBUTION / AVAILABILITY STATEMENT Approved for public release; distribution is unlimited.					
13. SUPPLEMENTARY NOTES ¹ National Research Council Postdoctoral Research Associate					
14. ABSTRACT The reduction of oxygen concentration in graphene oxide is demonstrated using electron beam generated plasmas produced in three different gas backgrounds: Ar, Ar/H ₂ and Ar/CH ₄ . Plasma diagnostics and surface characterizations are combined to determine the influence of each working gas on the chemical composition and structure of graphene oxide before and after reduction. The results suggest that argon treatment alone allows the removal of weakly bound oxygen in graphene oxide by inert ion bombardment, while the addition of hydrogen adds reactive species that enhance the removal of oxygen. However, without a carbon source, removing oxygen from graphene oxide can lead to the formation of defects and vacancies. We find that methane provides not only hydrogen but also the carbon necessary to restore the graphitic plane by healing defects generated during reduction.					
15. SUBJECT TERMS Graphene oxide Argon Reduction Hydrogen Plasma Methane					
16. SECURITY CLASSIFICATION OF:			17. LIMITATION OF ABSTRACT Unclassified Unlimited	18. NUMBER OF PAGES 9	19a. NAME OF RESPONSIBLE PERSON Scott G. Walton
a. REPORT Unclassified Unlimited	b. ABSTRACT Unclassified Unlimited	c. THIS PAGE Unclassified Unlimited			19b. TELEPHONE NUMBER (include area code) (202) 767-7531

1. Introduction

Graphene, the two-dimensional sp^2 bonded carbon sheet, has attracted much attention for its outstanding properties. One of the routes to large-area synthesis of graphene, or at least graphene-like material, is by reducing the oxygen concentration in graphene oxide (GO). GO is produced through a derivative of the well-known oxidation method of graphite described by Hummers and Offeman [1], which yields a solution of GO flakes that can be readily spin cast over large, arbitrary substrates. Fully oxidized GO is an insulator. However, it has been shown that by controlling the oxygen concentration, one can tune its electrical conductivity [2-4]. Different techniques can reduce graphene oxide including wet approaches using for example, solutions of hydrazine hydrate [5] or dry processes like heating [6,7] and plasma techniques [8-10]. Plasmas are the tool of choice across a broad range of industries given their ability synthesize and modify materials over large areas with nanoscale precision. Surface modification is of particular interest for making physical and chemical changes in the top few layers of materials while maintaining the properties of the bulk. When plasma processing atomically thin films like GO, considerable care must be taken to prevent any etching of the material. For such films, electron beam generated plasmas are ideal due to their high plasma densities and inherently low electron temperatures, which results in a large flux of low energy ions at substrate surfaces. Typical ion kinetic energies do not exceed a few eV [11,12] which is insufficient energy to sputter surface atoms but enough to promote surface diffusion and stimulate desorption [13].

In previous work [10], X-ray photoelectron spectroscopy (XPS) results demonstrated the ability to cleanly and controllably reduce the oxygen concentration in GO from 45 at.% to 5 at.% using electron-beam generated plasmas produced in argon/methane (Ar/CH₄) backgrounds. However, unlike other reduction approaches [14] the process was found to increase the sp^2 cluster size. The present work clearly delineates the role of a carbon-rich background gas in preserving the graphitic plane from defects during the reduction process by comparing the results using electron beam generated plasmas produced in Ar, Ar/H₂ and Ar/CH₄ to reduce GO. The treated material was characterized to follow the chemical and structural changes using surface energy measurements as well as X-ray photoelectron and Raman spectroscopies. To draw further distinctions between the various background gases, we measure plasma densities and relative ion fluxes to adjacent surfaces in each background. The results provide additional insight and support the general argument that a carbon-rich working gas, in this case methane, delivers carbon to the surface and is thus a better choice for reduction in terms of the physico-chemical characteristics of the reduced graphene oxide.

2. Experimental

The experimental detail of the plasma processing system and the reduction protocol has been described elsewhere [10]. Briefly, the system employs a sheet-like, pulsed, high-energy (≈ 2 keV) electron beam that ionizes and excites the background gas to produce plasma. The electron beam is collimated with a 150 Gauss magnetic field to provide a well-defined and localized ionization volume.

The graphene oxide films were produced by the Hummers method [1] and dispersed in water by sonication. The solution was then spin cast on SiO₂ (300 nm)/Si substrates and

dried in nitrogen. The samples were then placed on a stage located 2.5 cm from the electron beam axis and the system was evacuated to a base pressure of $<10^{-5}$ Torr. Plasma processing was performed at 90 mTorr pressure, which was achieved by introducing the gases through mass flow controllers and by throttling the turbo-molecular pump. Argon was the main constituent of the process environment with reactive gases (H_2 or CH_4) set to 5% of the total gas flow. The samples were treated for 5 minutes at a 10% duty factor (2 ms pulse width and a period of 20 ms), which is equivalent to 30 seconds of plasma exposure.

After plasma treatment, the samples were characterized and compared using Raman spectroscopy and X-ray photoelectron spectroscopy (XPS). The contact angles of three liquids—deionized distilled water, ethylene glycol and diiodomethane—were measured to determine the components of the surface energy following the method of Owens and Wendt [15], where the relation between the contact angle and the surface energy is described by:

$$\gamma_L(1 + \cos \theta) = 2 \left(\sqrt{\gamma_S^d \gamma_L^d} + \sqrt{\gamma_S^p \gamma_L^p} \right),$$

with

$$\gamma_S = \gamma_S^d + \gamma_S^p,$$

where θ is the measured equilibrium contact angle of the liquid on the surface, γ_S is the surface energy of the surface to be measured, γ_L is the surface tension of the used liquid, and the super scripts d and p indicate the dispersive and polar components of the surface and liquid energy or tension, respectively. Thus, knowing the surface tensions of the three liquids, and their polar and dispersive components, the measured contact angles can be used to derive the total surface energy and its polar and dispersive components. For this work, the average contact angle of three to five drops was used.

To understand the relative production of species and their transport to surfaces in the different gas backgrounds, measurements of plasma densities and relative ion fluxes at an adjacent surface were measured in a similar system [16]. Although the system is different than the one used for processing, the salient physics is the same. That is to say, the relative production of species via high-energy electron beams will depend largely on three parameters: beam energy, operating pressure, and relative gas concentration [12]. These three parameters were nominally the same in each system. For these measurements a 1 cm diameter, high-energy (2 keV) electron beam was injected into Ar, Ar/ H_2 and Ar/ CH_4 gas mixtures. The total flow was 100 sccm and the pumping speed was throttled using a manual gate valve to set the pressure at 90 mTorr. For the mixtures, the H_2 and CH_4 flow rates were set to 5% of the total flow (5 sccm) with the remainder being argon. Langmuir probes were used to measure the electron density as a function of distance from the beam axis. The ion fluxes were measured using an energy-resolved mass spectrometer (Hiden Analytical) located approximately 2.5 cm from the beam axis. Details of these measurement techniques can be found in [17].

3. Results and discussion

The differences in species production in the gas backgrounds used for processing can be seen in Figures 1 and 2. From Figure 1, the on-axis (position = 0 cm) electron density is

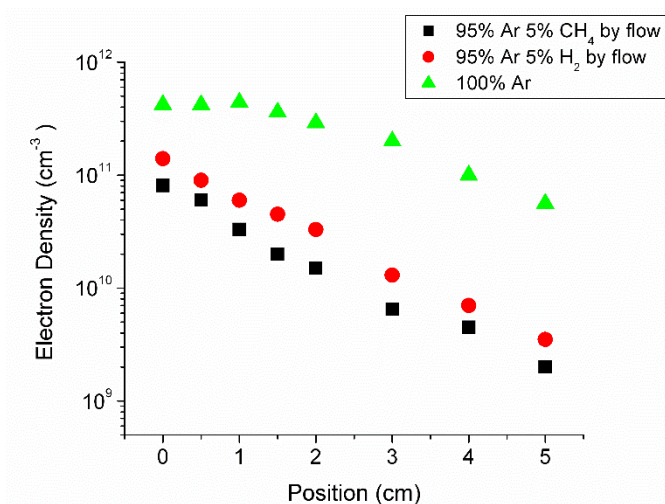


Figure 1 Electron density as a function of distance from the electron beam axis. The total flow was 100 sccm and the total pressure was 90 mTorr for all gas mixtures.

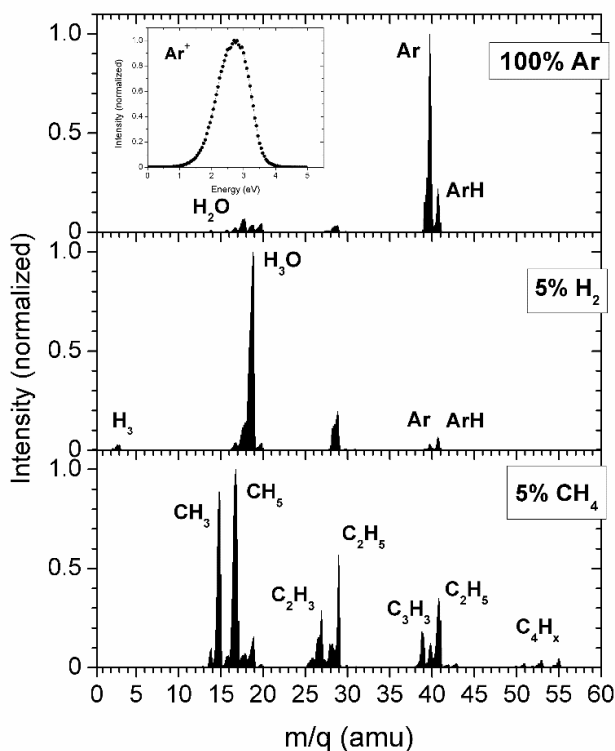


Figure 2 The ion mass spectrum measure at an electrode located 2.5 cm from the beam axis. The flow and pressures were the same as in Figure 1. The inset shows an ion energy distribution typical for all conditions.

found to decrease when molecular gases are added and the density drops more rapidly with increasing distance from the beam. This is not surprising since the primary loss mechanism is diffusion to the wall in beam generated plasmas produced in noble gas backgrounds; electron-ion recombination (e.g. $\text{H}_2^+ + \text{e}^- \rightarrow 2\text{H}$) in the bulk plasma adds an additional loss channel when molecular gases are introduced [18].

From Figure 2, the ion mass spectrum in pure argon is dominated by Ar^+ ions. The ArH^+ and water ions are indicative of residual water present in the reactor. When H_2 is added to the background, the Ar^+ ion intensity drops significantly, a large H_3O^+ signal emerges, and traces amounts of H_3^+ are observed. Molecular gases (in this case H_2) readily undergo charge exchange reactions with noble gas ions (e.g. $\text{Ar}^+ + \text{H}_2 \rightarrow \text{ArH}^+ + \text{H}$), with other molecular gases (e.g. $\text{H}_2^+ + \text{H}_2\text{O} \rightarrow \text{H}_3\text{O}^+ + \text{H}$), or themselves ($\text{H}_2^+ + \text{H}_2 \rightarrow \text{H}_3^+ + \text{H}$). Considering these charge exchange reactions, the aforementioned electron ion recombination reaction, and direct dissociation of H_2 from high-energy beam electrons implies that, despite the relatively low H_2 neutral density, a significant amount ionic H-containing species (as well as reactive neutrals) will be produced and delivered to the surface. When H_2 is replaced by CH_4 , a significant number of C_xH_y^+ ion species are observed. While the myriad of reactions leading to the measured spectrum are rich in gas-phase chemistry and certainly worthy of

continued investigations, the relevant result to this work is that there are an abundance of carbon-containing ions and presumably neutral radicals that are created and delivered to the graphene oxide surface.

The relevant characteristics of graphene oxide, GO reduced in Ar-produced plasmas (Ar-rGO), GO reduced in Ar/H₂-produced plasmas (H₂-rGO) and GO reduced in Ar/CH₄-produced plasmas (CH₄-rGO) are compared in Table 1. The surface energy is clearly modified after plasma treatment and is dependent on the working gas. Generally, the addition of oxygen to a surface will increase the surface energy, transforming the surface from hydrophobic to hydrophilic and thus increasing reactivity. The plasma treatment does not change the dispersive component of the surface energy. This is expected since the plasma treatment changes the concentration of the polar functional groups containing oxygen on the graphene surface. Ar plasma treatment has little effect on the polar component. However, the addition of reactive gases leads to substantial reduction in the polar component and thus the total surface energy. The CH₄-containing plasma produces the largest decrease, bringing the total surface energy to 45.5 mJ/m². These results are similar to those found for hydrazine-reduced graphene oxide, where the value was decrease from 62.1 mJ/m² to 46.7 mJ/m² [19]. The XPS survey results in Table 1 verify that the reduction in surface energy is linked to the decrease in the oxygen concentration. A slight decrease of the oxygen concentration was achieved using argon plasmas while the reduction of oxygen using reactive gas-containing plasmas was substantial.

Table 1 Surface energy calculated from the contact angle measurments of three liquids on untreated and plasma-treated graphene oxide and the corresponding oxygen concentration and oxygen-to-carbon ratio.

Quantity		GO	rGO Ar plasma	rGO Ar/H ₂ plasma	rGO Ar/CH ₄ plasma
Surface Energy (mJ/m ²)	Polar	25	24	16	7.5
	Dispersive	36	35	36	38
	Total	61	59	52	45.5
O concentration (at.%)		43	36	30	10
O/C ratio		0.75	0.56	0.43	0.1

The results of the oxygen reduction are best detailed by looking at the C1s high resolution XPS spectra shown in Figure 3. Fitting results show the presence of C-C, C-O, C=O and O-C=O bonds at 284.4 eV, 286.5 eV, 287.6 eV and 288.8 eV, respectively. Their concentrations are shown in Figure 4. For all processing conditions, the C-C concentration clearly increases and is accompanied by the decrease of C-O concentrations. These species can be located either on the basal plane or along the edges of the GO flakes [21]. The contributions from the O-C=O and the C=O peaks, attributed to species mainly located at the GO edges [20], changed only slightly when using pure Ar and Ar/H₂ plasmas. However, the use of CH₄ clearly enhances their reduction. It is important to note that the deposition of amorphous carbon using methane has been ruled out for the treatment conditions in this work [10].

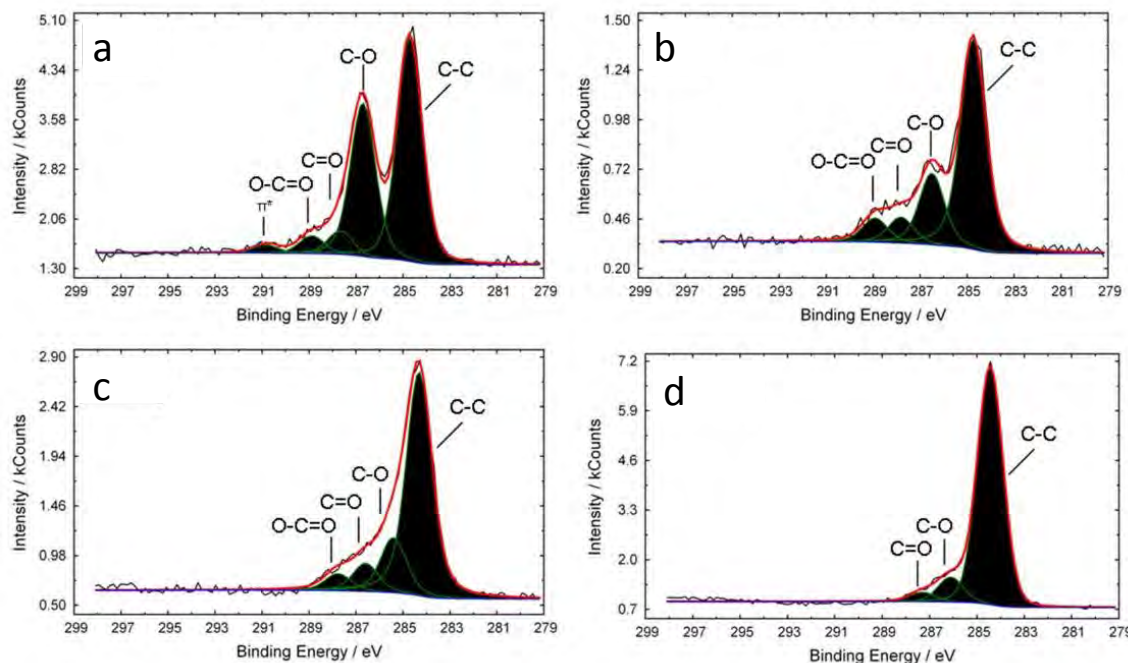


Figure 3 C1s XPS high resolution spectra of (a) GO and its plasmas reduced counterparts: (b) Ar-rGO, (c) Ar/H₂-rGO and (d) Ar/CH₄-rGO.

Following our earlier observation that sp^2 cluster size increased when reducing GO in Ar/CH₄ plasmas, [10] we measured the D to G ratios using Raman spectroscopy to calculate the sp^2 cluster size (L_a) using the empirical formula: L_a (nm) = $10^3 / (227 \cdot I_D/I_G)$ of Tuinstra and Koenig [21]. Those results are presented in Figure 5. In contrast to the results using Ar/CH₄ plasmas, the D to G ratio, and consequently the sp^2 cluster size decreased or remained constant for GO treated in Ar and Ar/H₂ plasmas.

The results indicate that argon plasmas can reduce the oxygen content. That is, a flux of non-reactive, low energy ions are sufficient to remove weakly bound oxygen (C-O). The addition of charged and neutral hydrogen species enhances the reduction. This is not

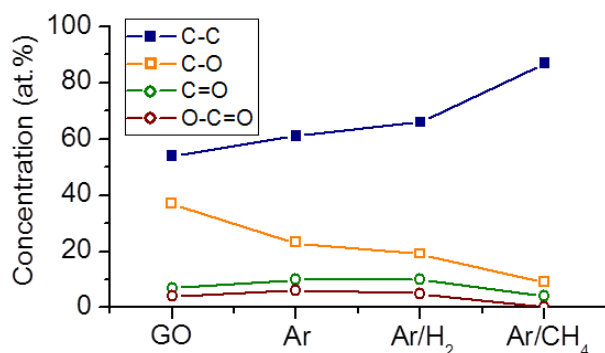


Figure 4 Concentration of carbon components from the C1s spectra of figure 3 for GO and rGO treated in Ar, Ar/H₂ and Ar/CH₄ gas mixtures.

surprising given the addition of H can produce volatile species like H₂O or OH, thus making the removal of oxygen easier. It is well known that the defect sites of graphene are more reactive than the carbon in the plane [22], and so the interaction of the species takes place mainly on the edges and at defect sites. However, the removal of oxygen in itself can create a defect, either by leaving a dangling bond or through the simultaneous removal of carbon via, for example,

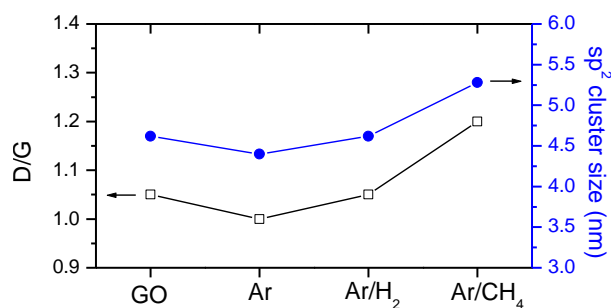


Figure 5 D to G intensity ratio and sp^2 cluster size of GO and r-GO plasma treated in Ar, Ar/H₂ and Ar/CH₄ gas mixtures.

in carboxyl and carbonyl groups (Figure 4) and an increase in the sp^2 cluster size of Ar/CH₄-rGO over both Ar-rGO and Ar/H₂-rGO (Figure 5).

4. Summary

The final oxygen content and surface structure of GO when using electron beam produced plasmas to reduce the oxygen content is strongly dependent on the type of background gas. Argon plasmas provide an inert flux of low energy ions capable of removing a small amount of oxygen, while the addition of hydrogen can stimulate a further reduction of oxygen content via the delivery of hydrogen-containing species. The addition of methane will stimulate further reduction. But, unlike hydrogen plasmas, those generated in methane backgrounds produced a wide range of carbon- and hydrogen-containing species, where the additional carbon could fill vacancies created by the removal of oxygen.

Acknowledgement

This research was supported by the Naval Research Laboratory base program. M.B. appreciates the support of the National Research Council.

References

- [1] Hummers WS, Offeman RE (1958) Preparation of graphitic oxide. *J. Am. Chem. Soc.* 80:1339–1339.
- [2] Jung I, Dikin DA, Piner RD, Ruoff RS (2008) Tunable electrical conductivity of individual graphene oxide sheets reduced at “low” temperatures. *Nano Letters* 8:4283–4288.
- [3] Eda G, Fanchini G, Chhowala M (2008) Large-area ultrathin films of reduced graphene oxide as a transparent and flexible electronic material. *Nature nanotechnology* 3:270–275.
- [4] Mattevi C, Eda G, Agnoli S, Miller S, Mkhoyan KA, Celik O et al. (2009) Evolution of electrical, chemical, and structural properties of transparent and conducting chemically derived graphene thin films. *Advanced functional materials* 19:2577–2584.
- [5] Stankovich S, Dikin DA, Piner RD, Kohlhaas KA, Kleinhammes A, Jia Y et al. (2007) Synthesis of graphene-based nanosheets via chemical reduction of exfoliated graphite oxide. *Carbon* 45:1558–1566.

the desorption of CO or CO₂; those defects could be passivated by the uptake of oxygen upon exposure to air.

When the plasma is produced in the presence of methane instead of hydrogen, hydrogen species are still produced and delivered to the surface. In addition, C_xH_y species are present and provides carbon that can heal vacancies created by the removal of oxygen. This concept is consistent with noticeable reduction

- [6] Yang D, Velamakanni A, Bozoklu G, Park S, Stoller M, Piner RD et al. (2009) Chemical analysis of graphene oxide films after heat and chemical treatments by X-ray photoelectron and Micro-Raman spectroscopy. *Carbon* 47:145–153.
- [7] Wei Z, Wang D, Kim S, Kim S, Hu Y, Yakes MK et al. (2010) Nanoscale tunable reduction of graphene oxide for graphene electronics. *Science* 328(5984):1373-1377.
- [8] Gomez-Navarro C, Weitz RT, Bittner AM, Scolari M, Mews A, Burghard M, et al. (2007) Electronic transport properties of individual chemically reduced graphene oxide sheets. *Nano Lett* 7(3):499–504.
- [9] Cardinali M, Valentini L, Fabbri P, Kenny JM (2011) Radiofrequency plasma assisted exfoliation and reduction of large-area graphene oxide platelets produced by a mechanical transfer process. *Chemical Physics Letters* 508:285–289.
- [10] Baraket M, Walton SG, Wei Z, Lock EH, Robinson JT, Sheehan PE (2010) Reduction of graphene oxide by electron beam generated plasmas produced in methane/argon mixtures. *Carbon* 48:3382-3390.
- [11] Walton SG, Muratore C, Leonhardt D, Fernsler RF, Blackwell DD, Meger RA (2004) Electron-beam-generated plasmas for materials processing. *Surface & Coatings Technology* 186:40-47.
- [12] Walton SG, Boris DR, Hernández SC, Lock EH, Petrova TzB, Petrov GM, and Fernsler RF (2015) Electron Beam Generated Plasmas for Ultra Low Te Processing. *ECS J. Solid State Sci. Technol.* 4: N5033-N5040.
- [13] Hess DW, Graves DB (1989) In *Microelectronics Processing: Chemical Engineering Aspects*. Washington, DC: American Chemical Society.
- [14] Cuong TV, Pham VH, Tran OT, Hahn SH, Chung JS, Shin EW et al. (2010) Photoluminescence and Raman studies of graphene thin films prepared by reduction of graphene oxide. *Materials Letters* 64:399–402.
- [15] Owens DK, Wendt RC (1969) Estimation of the surface free energy of polymers. *J Appl Polym Sci* 13:1741-1748.
- [16] Boris DR, Petrov GM, Lock EH, Petrova Tz.B, Fernsler RF, Walton SG (2013) Controlling the electron energy distribution function of electron beam generated plasmas with molecular gas concentration: part I. experimental results. *Plasma Sources Sci. Tech.* 22: 065004-6.
- [17] Boris DR, Fernsler RF, Walton SG (2015) Measuring the Density, Electron Temperature, and Electronegativity in Electron Beam Generated Plasmas Produced in Argon /SF₆ Mixtures. *Plasma Sources Sci. Tech.* 24, 025032-6.
- [18] Boris DR, Fernsler RF, Walton SG (2014) The spatial profile of density in electron beam generated plasmas. *Surf. Coat. Tech.* 241, 13-18.
- [19] Wang S, Zhang Y, Abidi N, Cabrales L. (2009) Wettability and Surface Free Energy of Graphene Films. *Langmuir*; 25(18):11078–11082.
- [20] Gao X, Jang J, Nagase S. (2010) Hydrazine and thermal reduction of graphene oxide: Reaction mechanisms, product structures, and reaction design. *J. Phys. Chem. C* 114:832–843.
- [21] Tuinstra F, Koenig JL (1970) Raman spectrum of graphite. *J Chem Phys* 53:1126–1156.
- [22] Wang X, Tabakman SM, Dai H (2008) Atomic layer deposition of metal oxides on pristine and functionalized graphene. *J. Am. Chem. Soc.* 130:8152–8154.

